Feature Extraction and Area Identification of Wireless Channel in Mobile Communication

Jie Li, Liyan Zhang, Xiaojian Feng, Kuankuan Jia, Fanbei Kong

Laboratory of Engineering Computing, North China University of Science And Technology, China
{lijie-2573017, zhangly_ncst}@163.com, njnufxj@126.com, {KuankuanJia_ncst, fbkong_ncst}@163.com

Abstract

The rapid development of mobile communication industry has exerted great influence on human life and social development. The uniqueness of mobile communication comes from wireless channels. The wireless channel may have some different feature in different scenarios or regions. It is a hot topic to analyze and extract these characteristics.

The measured wireless channel data for three different scenarios are analyzed in this paper. Firstly, the influence of noise and filter on the measurement signal is analyzed. Secondly, the characteristics of envelope statistics, autocorrelation function, multipath intensity distribution function, Doppler power spectrum and time interval correlation function of wireless channel are studied and the new parameters are defined according to the filter characteristics. The differences of these parameters in different scenes are studied, and the required "fingerprint" features are extracted.

In this paper, SVM is the basic unit of classifier to solve the problem of recognition and clustering of wireless channel scenes. Using the channel "fingerprint" feature extracted from different scenes to train the SVM model, and using bayesian posterior probability as the criterion, the recognition of the scene can be realized accurately. The adjacent segment clustering algorithm based on SVM can classify the channel paragraphs after segmentation.

Keywords: The wireless channel, Feature extraction Support Vector Machine, Adjacent segment clustering

1 Introduction

The mobile communication industry has been developing rapidly at an alarming rate. It has become one of the major high-tech industries that drive the development of the global economy. In mobile communication, the wireless channel is the transmission medium of electromagnetic wave propagation between the transmitter and receiver of the wireless communication system [1]. The research on the transmission characteristics of wireless channels and the establishment of an accurate wireless channel communication model are the prerequisites for the study of wireless broadband access and wireless communication system design. The wireless channel model affects the transmission rate and transmission quality of the entire wireless communication system directly [2].

Wireless channel is closely related to surrounding environment, and it has some characteristics in different environments. It is of great importance to the design of wireless devices and the optimization of wireless networks to use the mathematical methods to extract the characteristics of wireless channels. By analogy with human fingerprints, we describe the characteristics of the above wireless channel as wireless channel "fingerprint" [3]. The wireless channel "fingerprint" feature model has extracted the characteristics of wireless channels in different scenes or different regions on the basis of prior models and test data. It is of great significance to study the fingerprint characteristics of wireless channels in real environment.

The characteristics of wireless channel are the basis of wireless transmission technology. Many scholars at home and abroad carry out theoretical research and actual measurement of wireless channels and obtain many scientific achievements [4]. However, the wireless channel communication environment is complex and changeable, and there are still many problems to be solved. Research on the fingerprint characteristics of wireless channels is mainly to study the characteristics of environmental fingerprint, and some characteristics of differentiation [5].

Scene recognition or regional division based on the fingerprint model is significant for optimizing wireless network. We can find out the physical characteristics that reflect the uniqueness of wireless channel, and using it to accurately locate or detect sensitive environment [6].

*Corresponding Author: Liyan Zhang, Email: zhangly_ncst@163.com
DOI: 10.3966/160792642019032002021

2 Problem Formulation

In wireless channels, the transmission of electromagnetic waves is affected by the surrounding environment, and the path formed by scattering including reflection and diffraction is not singular [7]. Because the distance of electromagnetic wave propagation is different, the same transmission signals reach the receiving end at different times through each route, namely, there are differences in the time delay between the multiple diameters. In addition, the effects of each path on the same emission signal are different, there are differences between the coefficients of the multipath. As shown in Figure 1.

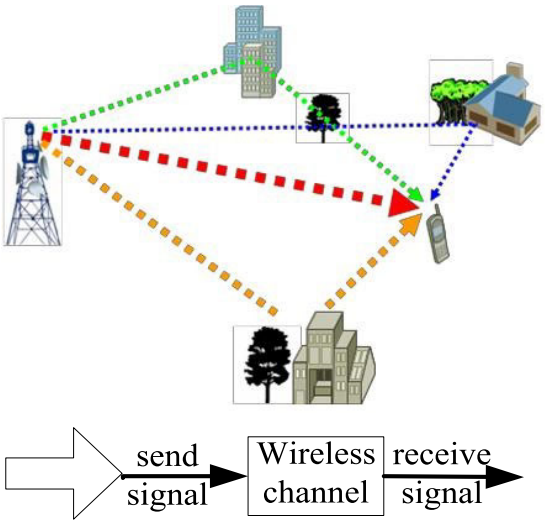

Figure 1. The multipath effect diagram of electromagnetic wave propagation

The transmission mechanism can be divided into three kinds: large scale decline, medium scale decline and small scale decline. The large scale propagation mechanism is used to describe the mean of the region. It has the propagation characteristic of the power law, which is that the power of the median signal is inversely proportional to the increase of the distance length [8]. Transmission mechanism of mesoscale describes the shadow fading, it is overlap in the large scale production potter on the median level of the average power of change, when expressed in decibels, this kind of change tends to be normal (gaussian) distribution, it is often referred to as lognormal shadows. And finally, the change in the signal envelope on the small scale is what describes a multipath fading, usually obeying the Rayleigh probability density function and is therefore also called Rayleigh fading. The fading classification of wireless communication channel is shown in Figure 2.

The time-varying characteristics of wireless channel are mainly reflected in the large scale decline and small scale decline, and the differences of wireless channels in different scenes and regions are mainly reflected in its small scale fading characteristics. The small scale

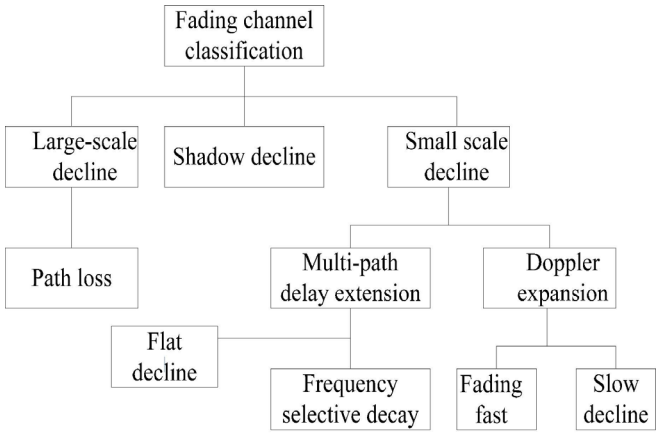

Figure 2. The channel fading classification diagram of wireless communication

decline of mobile communication is mainly composed of two parts: small scale fading based on multi-path delay expansion and small scale decline based on extension of time delay and doppler extension. The multipath effect allows the channel to generate time dispersion which can be described by the distribution of multi-diameter intensity. The time delay expansion is the time domain representation of time dispersion, and the parameters of the time dispersion are the average additional delay, the mean square root delay expansion and the coherence bandwidth. The doppler effect enables the time-varying characteristic channel to produce dispersion in frequency, which can be described by doppler power spectral density, and the parameters of frequency dispersion are described with doppler extension and coherence time.

In this paper, the multi-path strength distribution function of wireless channel and the doppler power spectral density function are established by analyzing the data of the measured channel, and the time dispersion parameters and frequency dispersion parameters are extracted. This paper analyzes the differences between different scenes and regional parameters, and uses the clustering algorithm based on SVM to identify the different "fingerprint characteristics".

3 Problem Solution

3.1 Feature Extraction

Filter and noise impact analysisSub-subsection. $c[k,n]$ stands for the measurement results of wireless channel after noise removal:

$$c[k,n]=\sum_{m=0}^{M-1}h[k-m,n]\cdot g[m]=h[k,n]*g[k] \quad (1)$$

$*$ means the convolution operation, g[k] means the filter equivalent function, g[m] means the filter coefficient.

The power spectrum density of c[k,n] is

$$\phi_c[\Delta f] = DFT\{h[k,n] * g[k]\} = \phi_h[\Delta f]\phi_g[\Delta f] \quad (2)$$

$\phi_g[\Delta f]$ represents the power spectral density function of $g[m]$. To simplify the analysis, the power spectral density of $g[m]$ only considers a low-pass filter with a bandwidth of 400Hz. As shown in Figure 3, the low-pass band approximation is flat. Therefore, when the channel impact response is filtered by the filter, the frequency interval correlation function only holds the inner part of [-200hz, 200Hz], and the rest is cut off. We can see from the above analysis, the filter impacts k-dimensional information of channel impulse response, and has no effect on n-dimensionaln information, but its power spectral density function within the bandwidth amplitude can reflect the multipath information. Therefore, in the following work, we mainly study the properties of filtered $c[k,n]$, and obtain the characteristic of channel impulse response $h[k,n]$.

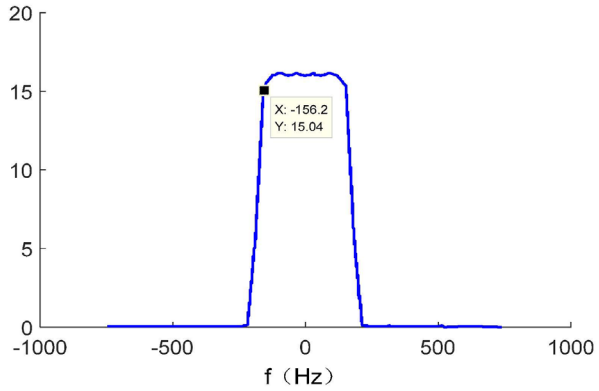

Figure 3. Filter power spectral density function

In addition, since the assumed noise is complex Gaussian white noise, which effect on the power spectral density of $C[k,n]$ is equivalent to adding a constant term and thus the analysis of multipath channel response has no effect on the characteristics of multipath and Doppler.

Envelope distribution characteristics analysis. Firstly, the amplitude characteristics of the measured data are analyzed to make the curve of the amplitude change at different times, as shown in Figure 4, there is no regular changes in amplitude were found [10].

Further, we normalize the amplitude, and divide the [0,1] interval by 100, to calculate the frequency of the amplitude and make the frequency curve of the amplitude, as shown in Figure 5.

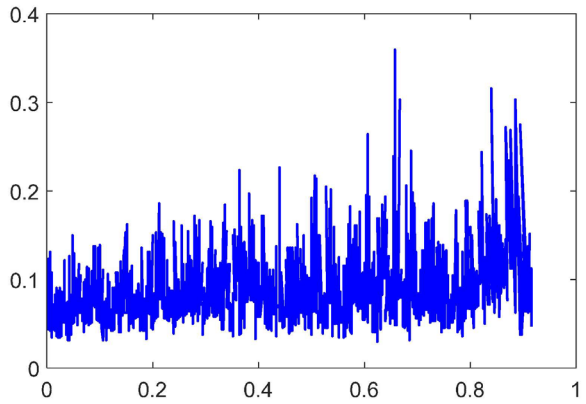

Figure 4. The amplitude varies from time to time

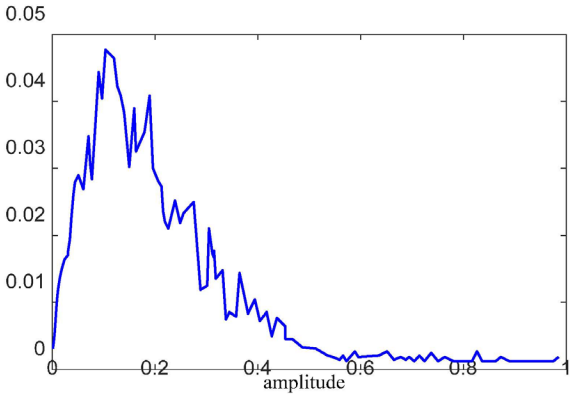

Figure 5. Amplitude curve

As we can see from the figure, the amplitude distribution is close to the Rayleigh distribution, so the maximum likelihood estimation is performed on the Rayleigh distribution parameters of the signal amplitude [11]. The probability density function of Rayleigh distribution is:

$$f(x) = \frac{x}{\sigma^2}\exp\left(-\frac{x^2}{2\sigma^2}\right), \quad x \geq 0 \quad (3)$$

The likelihood function is

$$L(x_1, x_2, \cdots x_n) = \prod_{i=1}^{n} f(x_i) = \frac{\prod_{i=1}^{n} x_i}{\sigma^2}\exp\left(-\frac{\sum_{i=1}^{n} x_i^2}{2\sigma^2}\right) \quad (4)$$

Taking the logarithm

$$\ln L = \sum_{i=1}^{n} \ln x_i - 2\ln\sigma - -\frac{\sum_{i=1}^{n} x_i^2}{2\sigma^2} \quad (5)$$

Seeking partial derivative

$$\frac{\partial \ln L}{\partial \sigma} = -\frac{2}{\sigma} + \frac{\sum_{i=1}^{n} x_i^2}{\sigma^3} \quad (6)$$

Making $\frac{\partial \ln L}{\partial \sigma}=0$, The maximum likelihood of getting σ is estimated to be

$$\hat{\sigma}=\sqrt{\frac{\sum_{i=1}^{n} x_i^2}{2}} \tag{7}$$

The probability density function of the Rayleigh distribution is shown in Figure 6, which is close to the amplitude frequency curve of the measured value.

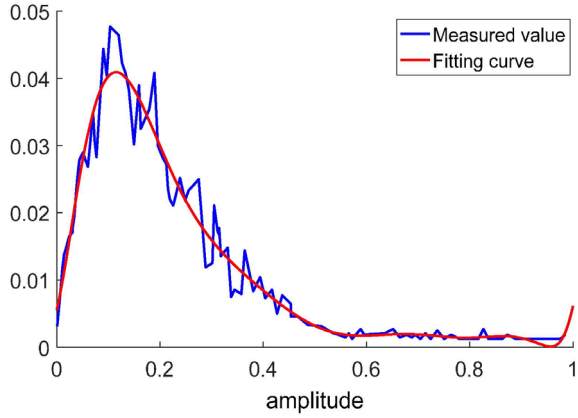

Figure 6. Rayleigh distribution probability density curve

The χ^2 goodness-of-fit test is used to test the fitting result and verify the measured signal amplitude conforms to the Rayleigh distribution. Supposing H_0: the distribution of the amplitude is Rayleigh distribution, the sample interval is [100] of [0,1], and the interval number is s = 100. Supposing that the number of samples in each interval is A_i and the total number of samples is n, the statistics χ^2:

$$\chi^2=\sum_{i=1}^{r}\frac{\left(N_i-np_i\right)^2}{np_i} \tag{8}$$

p_i is the probability of event A when the measured value Z_i obeys the assumed distribution :

$$p_i=\int_{a_i}^{a_{i+1}} f(x)dx \tag{9}$$

For a given level of significance, the goodness-of-fit test results are:

$\chi^2 < \chi_\alpha^2(s-r-1)$, the event of H_0 holds;

$\chi^2 \geq \chi_\alpha^2(s-r-1)$, the event of H_0 does not hold

The probability of P is obtained from the maximum likelihood estimation. Therefore, r = 1. In the case of significance level, the samples extracted from each scene measurement result are calculated and all the results satisfy the Rayleigh distribution. Therefore, all three scenes belong to the flat fading channel and there is no direct path.

Autocorrelation function. The autocorrelation function of signal c [k, n] is

$$\phi_c[k_1,k_2;\Delta n]=\frac{1}{2}E\left[c^*[k_1;n]\cdot c[k_2;n+\Delta n]\right] \tag{10}$$

In most wireless transmission media, the associated channel attenuation and phase shift with path delay K are irrelevant to the associated channel attenuation and phase shift with path delay D, so it can be assumed that the scattering of different delays is Irrelevant, the above becomes:

$$\phi_c[k;\Delta n]=\frac{1}{2}E\left[c^*[k;n]\cdot c[k;n+\Delta n]\right] \tag{11}$$

The autocorrelation function of the sample in each scene is as shown in the Figure 7:

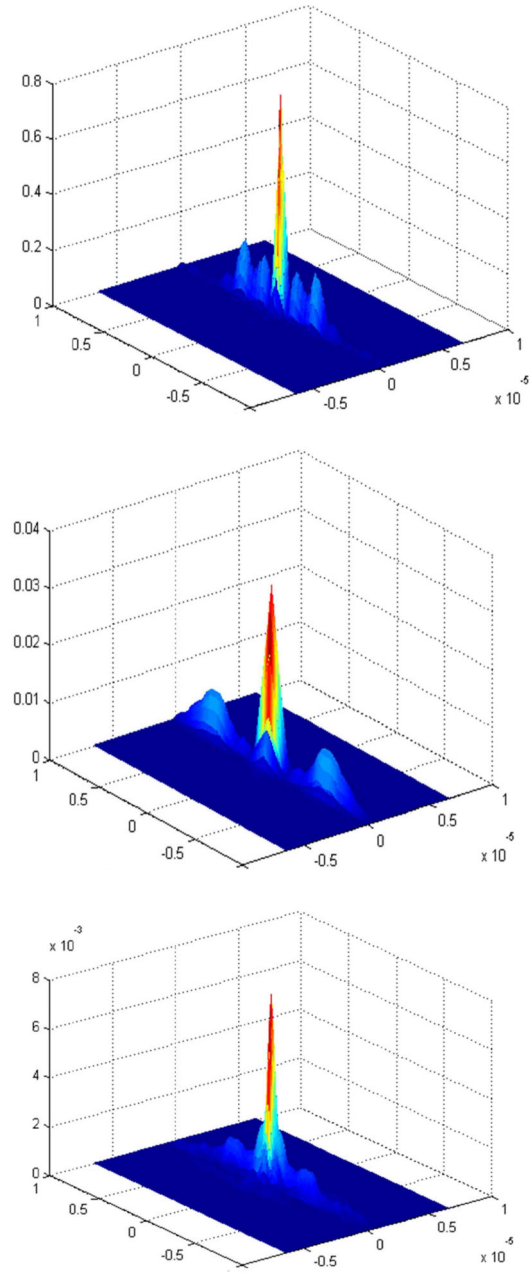

Figure 7. Autocorrelation function diagram

It can be seen that there are significant differences in the number and location of peaks in each scene. However, these differences can not be directly obtained, and the channel features need to be further extracted to characterize the characteristics of these differences and the physical meaning.

Multipath intensity distribution function. Making $\Delta n = 0$ to Produce multipath intensity distribution function $\phi_c[k] \equiv \phi_c[k;0]$

The range of k for which $\phi_c[k]$ is substantially non-zero is called channel multipath expansion named T_m.

The multipath intensity distribution function in each scene is shown in Figure 8 (Each scene selects a sample display, and the multi-diameter distribution function of the five samples in the same scene is similar).

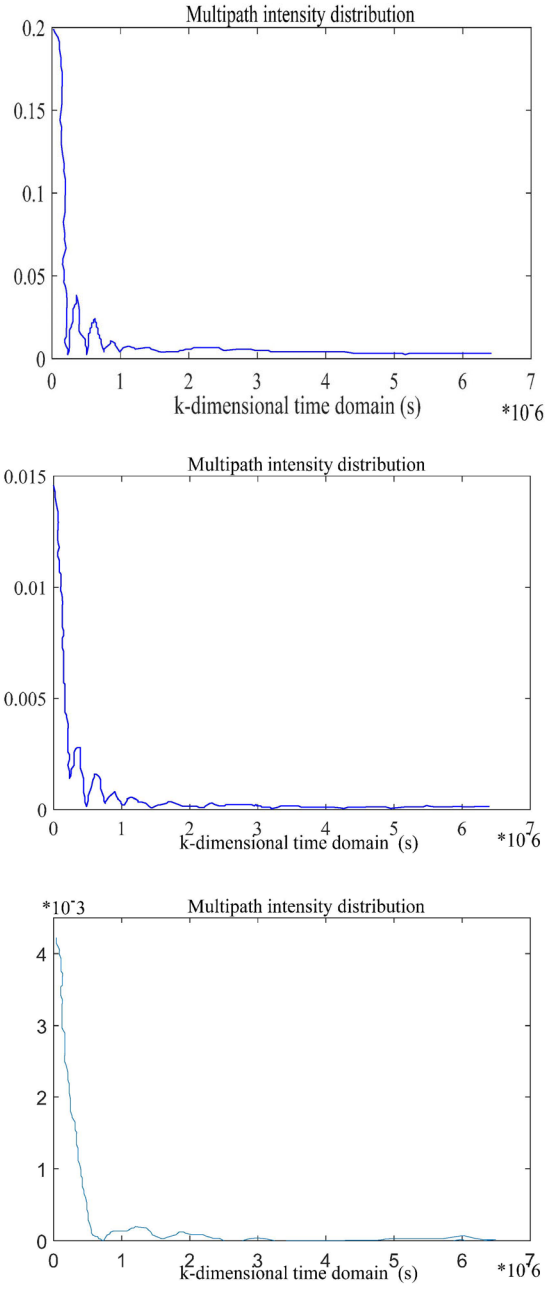

Figure 8. Multipath intensity distribution

It can be seen from the figure that the distributions of the multi-path intensities of scene 1 and scene 2 are close to each other, and scene 3 and scene 1, 2 differ greatly. The average additional delay $\bar{\tau}$ is expressed as

$$\bar{\tau} = E\{\tau\} = \int_0^\infty \tau P(\tau) dt \tag{12}$$

The root mean square delay extension σ_τ is expressed as

$$\sigma_\tau = \sqrt{\int_0^\infty (\tau - \bar{\tau})^2 P(\tau) d\tau} \tag{13}$$

the average additional delay $\bar{\tau}$ 、the root mean square delay expension σ_τ and the multi-path expansion T_m are shown in the table.

	Sample 1	Sample 2	Sample 3	Sample 4	Sample 5
Scene1	1.5531	1.5651	1.5638	1.5308	1.5532
Scene2	1.5416	1.5971	1.5329	1.5561	1.5521
Scene3	2.2634	1.6263	1.7162	1.8096	1.9753

Table 1. Root mean square delay expension σ_τ (10^{-13}s)

Multi-path expansion T_m (10^{-7}s)

	Sample 1	Sample 2	Sample 3	Sample 4	Sample 5
Scene1	1.4029	1.2344	1.3553	1.7050	1.1975
Scene2	2.1327	1.5391	1.9425	1.8072	1.4668
Scene3	0.4705	0.7333	0.5281	0.3336	0.4566

The average additional delay $\bar{\tau}$ (10^{-7}s)

	Sample 1	Sample 2	Sample 3	Sample 4	Sample 5
Scene1	1.7606	1.6402	1.7068	1.9126	1.6097
Sccne2	2.1896	1.8004	1.6452	1.4355	1.8266
Sccne3	0.5637	1.2758	0.8828	0.5133	0.6063

It can be seen from the table that the average additional delay $\bar{\tau}$ is basically smaller than that of scene 1 and scene 2 in scene 3, but scene 1 and 2 are indistinguishable; the root mean square delay expansion σ_τ is obviously smaller than scenes 1 and 2 in scene 3, 1 and 2 are indistinguishable; the multipath extension T_m is larger in scene 3 than scenes 1 and 2, but scenes 1 and 2 are indistinguishable. Therefore, the root mean square delay extension σ_τ can be used as a "fingerprint" feature to distinguish between Scene 3 and Scene 1 and Scene 2.

Doppler power spectrum. Taking Δn as a variable to $\phi_c[k;\Delta n]$ Fourier transform, get the scattering function $S[k;\lambda]$

$$S[k;\lambda] = \int_{-\infty}^{\infty} \phi_c[k;\Delta n] e^{-j2\pi\Delta n} d\Delta n \tag{14}$$

Taking k as a variable to $S[k;\lambda]$ Fourier transform, get the function $S_c[\Delta f;\lambda]$

$$S_c[\Delta f;\lambda]=\int_{-\infty}^{\infty}S[k;\lambda]e^{-j2\pi\Delta fk}dk \quad (15)$$

Geting the Doppler power spectrum:

$$S_c[\lambda]=S_c[0,\lambda] \quad (16)$$

The range in which the Doppler power spectrum $S_c[\lambda]$ is substantially a non-zero λ value is called the channel Doppler spread B_d. Define twice the average of the entire Doppler power spectrum as the lower threshold, which is used to calculate Doppler spread, ie, define the spectral width greater than the lower threshold as the Doppler spread. The calculation results are shown in the table below.

Table 2. Doppler expansion B_d (Hz)

	Sample 1	Sample 2	Sample 3	Sample 4	Sample 5
Scene1	142.6	134.6	120.1	191.1	170.6
Scene2	19	24.5	22	15	16.5
Scene3	10.2	3.5	15	15	16.5

As can be seen from the table. The Doppler spread of scene 2 and 3 is far than that of scene 1, while the difference between scenes 2 and 3 is not obvious. For the peak frequency, scenes 1 and 2 are relatively constant and easily distinguished, while the peak frequency of scene 3 varies greatly. Doppler spread and the number of peaks can be used as the "fingerprint" feature of the channel, and the peak frequency needs further analysis.

Doppler shift is caused by the relative movement of the receiving frequency, the principle shown in Figure. Assuming that the receiving station receives signals of far-field source, the receiving station is moving at a speed v, the distance in time Δt is d, and the distance plane wave reaches the direction of θ, then the distance difference between the two points is $\Delta l = v\Delta t\cos\theta/\lambda$ Doppler frequency shift is

$$f=\frac{1}{2\pi}\frac{\Delta\phi}{\Delta t}=\frac{v}{\lambda}\cos\theta \quad (17)$$

It is shown that doppler frequency shift is related to the movement speed and the Angle between movement direction and electromagnetic wave incident direction of the receiving station.

For scene 1, there are two Doppler shifts, and the frequency shift is basically constant, which shows that the moving speed of the receiving station in scene 1 is constant and there are two wireless channels whose angle with the moving speed is constant. For scene 2, there is a Doppler frequency shift, and the frequency shift is basically constant, which shows that the moving speed of the receiving station in scene 2 is constant and there is a wireless channel with a constant angle with the moving speed. For scene 3, there is a Doppler shift, and the frequency shift varies, reflecting the change of the moving speed of the receiving station in scene 3 or the change of the angle between the moving speed and the wireless channel.

According to the above analysis, the peak frequency is related to the speed of the receiving station and angle between the speed of movement and the channel, which may change for different samples in the same scene and can not be used as the "fingerprint" feature of the channel. However, for continuous scenes, the change is also Continuous and regular, which can be used as the channel "fingerprint" feature.

The number of Doppler shift peaks and the Doppler shift size obtained by the above method depend on the characteristics of the channel. The larger the number, the more Doppler peak information contains more detail information.

Time interval correlation function. Doing an inverse Fourier transform on the Doppler power spectrum $S_c[\lambda]$, and obtaining the time interval correlation function is $\phi C[\Delta n]$

$$\phi_c[\Delta n]=\int_{-\infty}^{\infty}S_c[\lambda]e^{-j2\pi\Delta n\lambda}d\lambda \quad (18)$$

Each scene time interval correlation function is shown in the Figure 9.

As can be seen from the diagram, the time interval correlation functions of the three scenarios are not very different, and the parameter coherence time from the graph is shown in Table 3.

As can be seen from the table, the correlation time of the three scenes is not regular, so correlation time can not be used as a "fingerprint" feature.

3.2 The Clustering Method Based on Support Vector Machine

Support vector machine (SVM) theory is derived from the support vector method that Vapnik proposed in 1963 to solve the problem of pattern recognition. This method mainly selects a set of characteristic subsets from the training set, so that the linear partition of the characteristic subset is equivalent to the segmentation of the whole dataset. This subset of features is called support vectors machine [12].

In this paper, the SVM method is used to treat the test data as follows:

According to the channel characteristics of the above analysis, to extract the autocorrelation function of the given data, doppler spectrum, the multipath intensity distribution function, time correlation function between "fingerprint" feature vector sequence $\{\hat{x}_n\}$, using the same method to extract the test data of the "fingerprint" feature vector sequence $\{\hat{T}_k\}$;

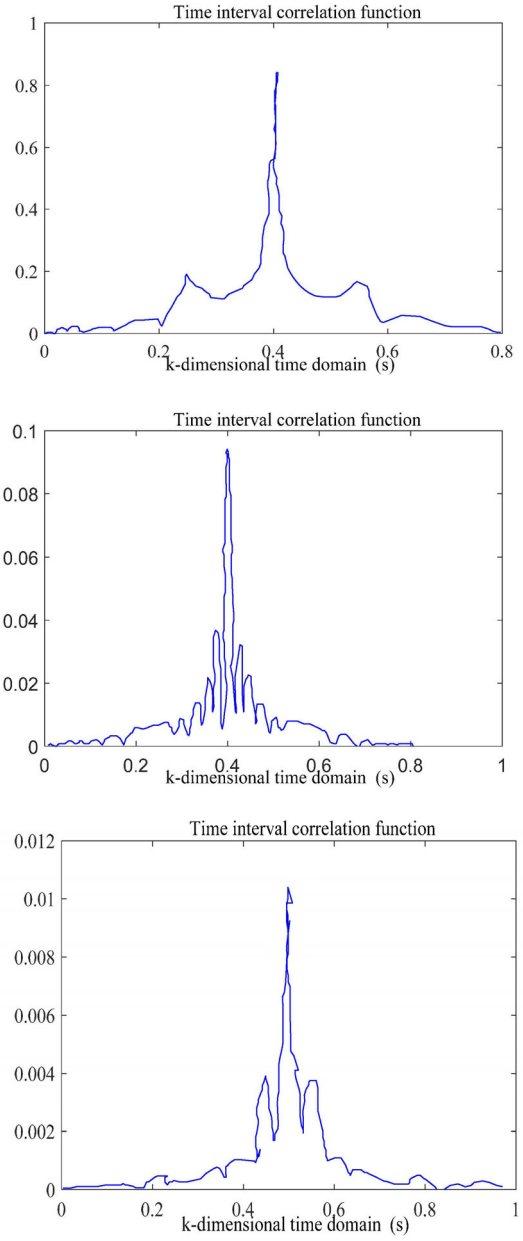

Figure 9. Time interval correlation function

Table 3. Parameter correlation time(s)

	Sample 1	Sample 2	Sample 3	Sample 4	Sample 5
Scene11	0.03987	0.07752	0.07133	0.06534	0.07734
Scene2	0.05066	0.04134	0.156	0.176	0.104
Scene3	0.1004	0.04666	0.02934	0.10134	0.032

The sequence $\{x_n, y_n\}$ is used as training data, which is the "fingerprint" feature vector sequence of scene 1~ 3, $y_i \in \{1,2,3\}$ which is the label of the subordinate scene, and constructs an optimal plane as follows:

$$x(\omega \cdot \hat{x}) + b = 0 \tag{19}$$

This optimal hyperplane has to satisfy the following constraints

$$y_i\left[x(\omega \cdot \hat{x}) + b = 0\right] \geq 1, \quad i = 1,2 \cdots N \tag{20}$$

At the same time, you should minimize the following function

$$\phi(\omega) = \frac{1}{2}\|\omega\|^2 = \frac{1}{2}(\omega \cdot \omega) \tag{21}$$

The optimal hyperplane form is as follows:

$$\sum_{SV} y_i a_i^0 (x \cdot x_i) + b_0 = 0 \tag{22}$$

The SVM is the support vector, a_i^0 is the Lagrange multiplier.

The "fingerprint" feature vector sequence $\{\hat{T}_k\}$ that is extracted from the test data can be substituted into the optimal hyperplane expression, which can be used to obtain the tag $\{\hat{L}_k\}$ of the scene of the test data that can identify the test data belongs to the scene. According to the output of SVM of support vector machine, the posterior probability of classification can be obtained by using bayesian formula. Samples by SVM output 1 or 0 process can be thought of as a binomial distribution, assuming that there are two kinds of general A and B, they take the sample of 1 s and 0 s prior probability of PA and 1 - PA and PB and PB respectively. The prior probability PA and PB can be obtained from the training samples A and B according to the trained SVM. Assuming that the new Data has N samples in Data, with the trained SVM to test Data, the number of outputs of 1 is N. According to bayes' formula:

$$\begin{aligned} P(A/n) &= \frac{P(A)P(n/A)}{P(A)P(n/A) + P(B)P(n/B)} \\ &= \frac{C_N^n P_a^n (1-p_a)^{N-n}}{C_N^n P_a^n (1-p_a)^{N-n} + C_N^n P_b^n (1-p_b)^{N-n}} \end{aligned} \tag{23}$$

In the N samples, the number of outputs of 1 is n after SVM, and the above formula gives the calculation formula of the posterior probability of Data belonging to the overall A.

After two or two matches of the scenario through SVM, you can infer the scenario of each set of data.

3.3 The Adjacent Segment Clustering Algorithm Based on SVM

Using the scale shrinkage time series segmentation algorithm based on temporal edge operator to section of "fingerprint" feature vector, get a set of time series segmentation results, all segments have their fingerprints, we can use the fingerprint similarity clustering segmentation for results, so as to get a reasonable "zoning". In order to cluster the segmentation results, we propose the clustering method based on SVM. The steps of this method are as follows:

(1) Each segment of the subdivision that will be obtained as a sample set is marked as $\{S_1, S_2 \cdots S_n\}$ in turn as shown in Figure 10. The matching results of the "fingerprint" feature vector sequences extracted from the test data are shown in the table.

S_1	S_2	S	…	S_i	S_i	S_{i+}	……	S

Figure 10. Step one

(2) Taking three samples sets $\{S_{i-1}, S_i \cdots S_{i+1}\}$ each time as the SVM cluster input, in which the sample set $\{S_{i-1}, S_{i+1}\}$ is the training sample and the sample set $\{S_i\}$ is the test sample for clustering

(3) If sample set $\{S_i\}$ and $\{S_{i-1}\}$ are more similar to the "fingerprint" eigenvector sequence, sample sets $\{S_i\}$ and $\{S_{i-1}\}$ are merged into $\{S_i\}$

(4) Repeating steps 2 and 3, and then take the sample sets $\{S_k\}$ for clustering as a test sample and the left and right adjacent sample sets $\{S_{k-1}, S_{k+1}\}$ as training samples and input the SVM for clustering, then do the merger to get the clustering result.

For the recognition and clustering of wireless channel scene, SVM is used as the basic unit of classifier. Using the channel "fingerprint" feature extracted from different scenes to train the SVM, and using bayes posterior probability as the criterion, the recognition of the scene can be realized. In order to complete the clustering of unlabeled channel scenes, we designed a clustering algorithm based on SVM, and realized the clustering and scene division of the segmented channel paragraphs. The above method is used to determine that the two sets of data are respectively in scenario 1 (probability is close to 100%) and scenario 2 (probability is 91.9%). The results show that SVM can effectively identify and cluster the scene of wireless channel according to the "fingerprint" feature extracted in this paper.

The adjacent segment clustering algorithm based on SVM achieves clustering and scene segmentation of the segmented channel segments. After the above process of modeling and analysis, it has some recognition to the feature extraction and recognition clustering of wireless channel, which is of great significance for analyzing wireless communication channel and improving the effect of wireless communication.

4 Conclusion

In this paper, various characteristics of measured channel data are extracted, refined and aggregated. After analyzing the real channel measurement results of different scenarios or environments, the differences of wireless channels in different scenarios and regions are obtained, which are mainly reflected in its small-scale fading characteristics and its fingerprints characteristics can be expressed by envelope distribution function, autocorrelation function, multipath intensity distribution function, Doppler power spectrum, and time interval correlation function. For the wireless channel scene recognition and clustering problems, the SVM is used as the basic unit of classifier. The SVM is trained by using the "fingerprinting" feature extracted from different scenes, and the Bayesian posterior probability is used as a criterion to identify the scene accurately. Adjacent segment clustering algorithm based on SVM achieves clustering and scene segmentation of the segmented channel segments.

Acknowledgments

This work was supported by the National Natural Science Foundation of China (No. 51674121), by the National Natural Science Foundation of Hebei Province (No. E2017209178), Science and technology project of Hebei province (No. 15214104D), the National Natural Science Foundation of Hebei Education Department (No. QN2016088), Graduate Student Innovation Fund of North China University of Science and Technology, Graduate Student Innovation Fund of Hebei Province (2017S03, CXZZSS2017071), and the outstanding youth fund project of North China University of Science and Technology (No. JQ201705).

References

[1] Z. Fu, H. Luo, P. Zerfos, The Impact of Multihop Wireless Channel on TCP Performance, *IEEE Transactions on Mobile Computing*, Vol. 4, No. 2, pp. 209-221, February, 2005.

[2] A. Konrad, B. Y. Zhao, A. D. Joseph, A Markov-Based Channel Model Algorithm for Wireless Networks, *Wireless Networks*, Vol. 9, No. 3, pp. 189-199, March, 2003.

[3] J. Ryckaert, P. Doncker, R. Meys, Channel Model for Wireless Communication around Human Body, *Electronics Letters*, Vol. 40, No. 9, pp. 543-544, September, 2004.

[4] H. J. Zhu, Y. K. Pei, J. H. Lu, Applying Fountain Codes in Deep Space Communication, *Journal of Internet Technology*, Vol. 9, No. 5, pp. 399-404, September, 2008.

[5] X. Yin, X. Zhou, Z. Li, S. Li, Joint Rate Control and Power Control for Lifetime Maximization in Wreless Sensor Ntworks, *Journal of Internet Technology*, Vol. 12, No. 1, pp. 69-78, January, 2011.

[6] Y. M. Baek, Current Status of E-commerce Market in China and Implication, *Journal of Digital Convergence*, Vol. 13, No. 1, pp. 111-124, January, 2015.

[7] C. Huang, Y. Feng, J. Zhao, Asymmetric Electromagnetic Wave Transmission of Linear Polarization via Polarization Conversion through Chiral Metamaterial Structures, *Physical*

Review B Condensed Matter, Vol. 85, No. 9, pp. 131-195, September, 2012.

[8] C. H. Lee, P. S. Mak, A. P. Defonzo, Optical Control of Millimeter-wave Propagation in Dielectric Wave Guides, *IEEE Journal of Quantum Electronics*, Vol. 16, No. 3, pp. 277-288, March, 1980.

[9] A. Lennie, S. Abdullah, Z. M. Nopiah, Behavioural Investigation of Fatigue Time Series using the Statistical Approach, *Journal of Applied Sciences*, Vol. 10, No. 16, pp. 1714-1722, December, 2010.

[10] L. Sboui, Z. Rezki, M. S. Alouini, Achievable Rate of Spectrum Sharing Cognitive Radio Systems Over Fading Channels at Low-Power Regime, *IEEE Transactions on Wireless Communications*, Vol. 13, No. 11, pp. 6461-6473, November, 2014.

[11] H. S. Wang, P. C Chang, On Verifying the First-order Markovian Assumption for a Rayleigh Fading Channel Model, *IEEE Transactions on Vehicular Technology*, Vol. 16, No. 1, pp. 353-357, January, 1996.

[12] T. S. Furey, N. Cristianini, N. Duffy, Support Vector Machine Classification and Validation of Cancer Tissue Samples Using Microarray Expression Data, *Bioinformatics*, Vol. 16, No. 10, pp. 14-906, October, 2000.

Biographies

Jie Li received a bachelor's and master's degree degree from hebei university of technology in 2005 and 2008. He received a doctorate from Northeastern University in 2015. He is an associate professor at north China university of science and technology. His research interests include mathematical modeling and metallurgical energy conservation.

Liyan Zhang is a Master student in the College of Science, North China University of Science and Technology, Hebei Tangshan, China. Her interests include numerical calculation, big data, mathematical modeling and high performance computing.

Xiaojian Feng received his M.Sc. degree in 2008 from Nanjing normal University, now he is lecturer in North China University of science and Technology. His main researche interests include Metallurgical Engineering and physics chemistry, etc.

Kuankuan Jia is an undergraduate student in the College of Information Engineering, North China University of Science and Technology, Hebei Province, China. His research interests include numerical calculation, big data, mathematical modelling and high-performance computing.

Fanbei Kong was born in Heze City, Shandong Province, China in 1996. He is an undergraduate student in the YiSheng College, North China University of Science and Technology, Hebei Province, China. His research interests include numerical calculation, big data, mathematical modelling and high-performance computing.